International Conference on Technologies and Materials for Renewable Energy, Environment and Sustainability, TMREES15

Comparison between Aggregation Techniques for PMSG Wind Farm

Mohammed. A. Badr[a], Ahmed. M. Atallah[b], Mona A. Bayoumi[c],[*]

[a]Electrical Engineering Department, Ain-Shames University, Cairo, Sbadr4446@yahoo.com, EGYPT
[b]Electrical Engineering Department, Ain-Shames University, Cairo, Atallah_eg@yahoo.com, EGYPT
[c]Electrical Engineering Department, Benha University, Benha, mona.elawa@bhit.bu.edu.eg, EGYPT

Abstract

This paper presents a wind farm composed of different permanent synchronous generator (PMSG) wind turbines (same wind turbine technology but different rated power or operational conditions) coupled to the same grid connection point. A comparison between the three techniques of wind farm aggregation for a farm composed of PMSG wind turbines. Our comparison is for the closeness of the results of normal and transient response of both the complete model and the aggregated models. The chosen three techniques are, multi full aggregated model using equivalent wind speed (MFAM-EWS), semi aggregated model (SAM) and mixed semi full aggregated model (MSFAM). Simulation has been carried out for these techniques by MATLAB/SIMULINK program to compare them with the complete model to prove the effectiveness of each aggregation technique.

Keywords: Wind power; aggregation model; PMSG.

* Corresponding author. Tel.: 00201283992983.
  E-mail address: mona.elawa@bhit.bu.edu.eg

1. Introduction

Wind power has an important role in the future energy in many regions across the world. Where wind energy is one of the most important permanent clean energy sources. The growing worldwide market will lead to further improvements, such as larger wind turbines and offshore wind farms. These improvements will lead to further cost reductions [1].

Modeling of wind farms for network integration studies is becoming an important issue. Increasing the number of wind turbines in the wind farm has increased farm size, thus simulating the whole wind farm by modeling each wind turbine separately leads to complexity and reduces the speed of the simulation. In order to reduce the computational time and the complexity, they [2,3,4,5] simplify the whole wind farm by aggregated wind farm model.

The aggregated wind farm represents full wind farm with groups of turbines or one single equivalent turbine. This aggregated model can first represent the behavior (active and reactive power exchanged with the grid) during normal operation characterized by small deviations and changes of wind speeds. Secondly, it represents the behavior of wind farm during grid disturbances, such as voltage drops and frequency deviations [2]. The aggregated wind farm represents the full reaction of wind turbines to any wind fluctuations and grid disturbances.

There are different wind turbine generator types, which have become widespread and commonly used in wind power. However, due to the attractive characteristics of permanent magnet synchronous generators such as noise reduction, higher reliability, gearless, higher efficiency, lower cost, and smaller size, the need to study the aggregated models with PMSG based wind turbines has increased [6]. Therefore, PMSG wind turbines have been traded by some WT manufactures, such as Siemens Power Generation, GoldWind and GE Energy.

This paper focuses on the comparison between the complete wind farm and some of aggregated models using MATLAB/SIMULINK program. The complete wind farm consists of different PMSG wind turbines (the same wind turbine technology but different rated power and operational points), experiencing different incoming wind speeds. The aggregated models that have been considered in this paper are; (1) multi full aggregated model using equivalent wind speed (MFAM-EWS), (2) semi aggregated model (SAM) and (3) mixed semi full aggregated model (MSFAM).

In this paper, we proposed large wind farm composed of different rated wind turbine of permanent magnet synchronous generators as shown in Fig. 1. We divide the wind farm to subgroups. Each group composed of almost the same rated power and operational conditions with different incoming wind speed. We aggregate each group and then aggregate the resultant groups as will be seen. We used the same techniques used with DFIG because it gave reasonable results. The power output of PMSGs behaves almost the same as DFIG except PMSG cut in speed is always lower than that of DFIG as depicted in Fig. 2 due to the nonexistence of gear box, which have zero efficiency at small wind speeds. Fig. 2 shows the power curve of 1.5 MW PMSG wind turbines [7].
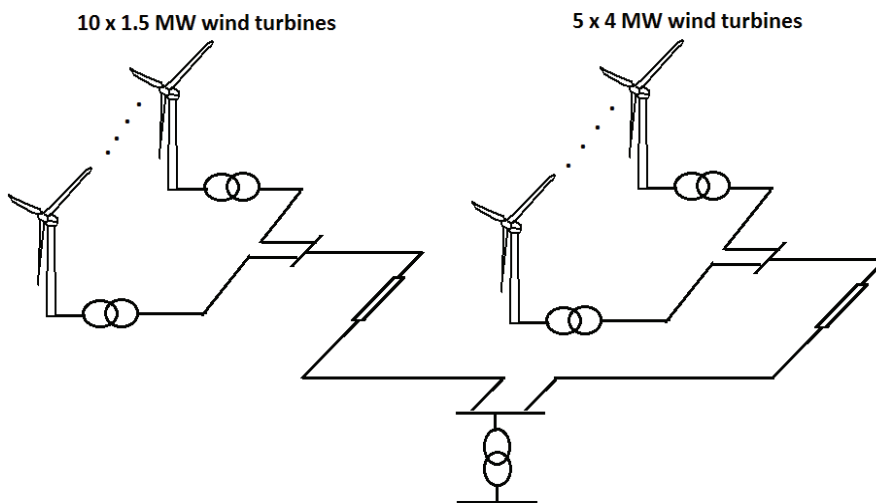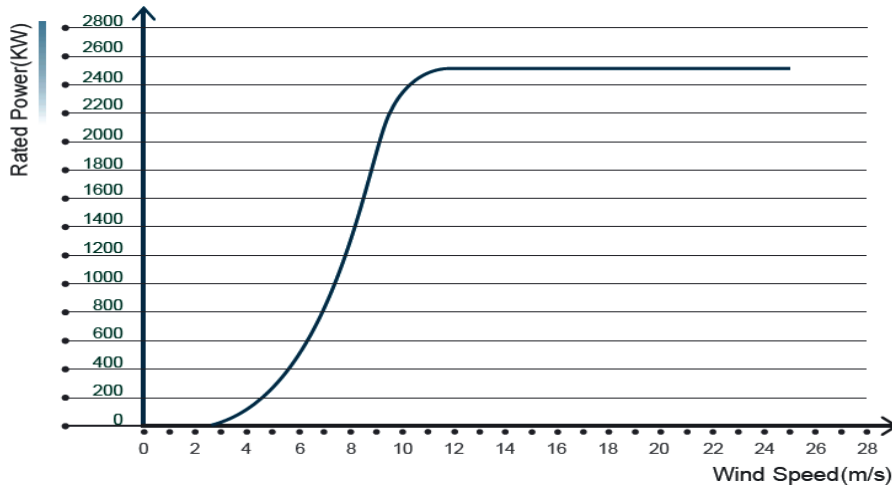

Fig. 1. PMSG wind farm structure.

Fig. 2. Dynamic power curve of GoldWind 1.5 MW PMSG wind turbine.

2. PMSG Wind Turbine Model

This paper uses 48 pole PMSG and back to back (B2B) Converter. Pulse width modulation (PWM) is used to produce the switching signals for converter switches. There is a braking resistor and capacitor between the two converters. Fig. 3 explains the general configuration of a PMSG system and we will study each component of the PMSG wind turbine.
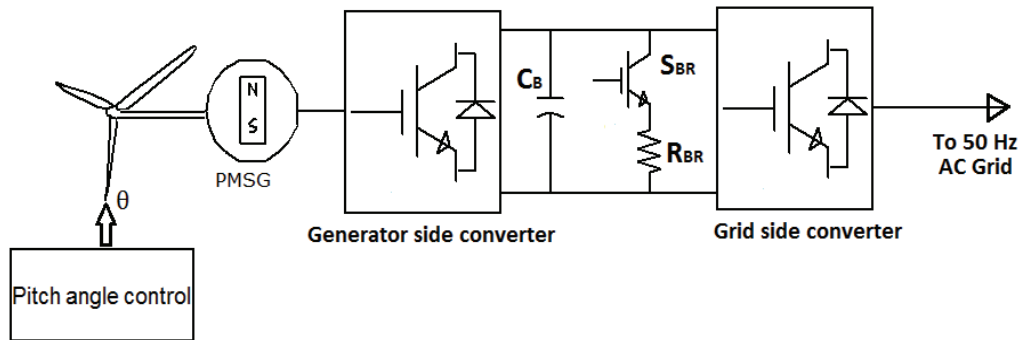

Fig. 3. Configuration of a PMSG wind turbine.

2.1. Aerodynamic model

The kinetic energy of the wind produces a mechanical torque is converted into the electric energy through generator. The aerodynamic power in the rotor of the turbine model is given by equation [8]:

$$P_{\omega} = 0.5 \rho A u^{3} C_{p}(\lambda, \theta) \tag{1}$$

where P_{ω} is the aerodynamic power, $\rho(\text{kg/m}^3)$ the air density, $A(\text{m}^2)$ the rotor swept area, $u(\text{m/s})$ the wind speed, and C_p the power coefficient as a function of the tip speed ratio λ and θ the pitch angle of rotor blades. The wind turbine can produce maximum power when the turbine operates at maximum C_p (i.e., at C_{p_opt}). Therefore, it is necessary to keep the rotor speed at an optimum value of the tip speed ratio λ_{opt}. If the wind speed varies, the rotor speed should be adjusted to follow the change [9].

2.2. Mechanical shaft modeling

The mechanical energy is transferred from the generator through the drive train. In multi pole PMSGs there is no need to gear box which allows to operate at low speeds, so the generator is connected directly to wind turbine.

The drive train is represented by one mass model, where all rotating masses are represented by only one element as depicted in the following equation [10]:

$$T_m - T_e = J_{eq} \frac{d\omega_r}{dt} \tag{2}$$

where T_m & T_e are the mechanical torque and electrical torque and J_{eq} is the equivalent inertia of the rotating system.

2.3. PMSG model

The dynamic model of the PMSG has been built in the d-q reference frame rotating at electrical speed with the position of the direct axis aligned along the permanent magnet flux position. The stator voltage equations in d-q reference frame have the following form [11]:

$$v_{sd} = -R_s i_{sd} - L_{sd} \frac{di_{sd}}{dt} + \omega_e L_{sq} i_{sq} \tag{3}$$

$$v_{sq} = -R_s i_{sq} - L_{sq} \frac{di_{sq}}{dt} + \omega_e \left(\psi_m - L_{sd} i_{sd} \right) \tag{4}$$

where v_{sd}, v_{sq} are the generator voltages, i_{sd} , i_{sq} , are the generator currents, R_s is the stator winding resistance, L_{sd}, L_{sq} are the stator inductances, Ψ_m is the magnet flux and ω_e is the generator angular speed.

The mechanical equation is described by the following electromagnetic torque equation:

$$T_e = \frac{3}{2} p \left(\psi_m i_{sq} + (L_{sd} - L_{sq}) i_{sd} i_{sq} \right) \tag{5}$$

As the PMSG uses a surface magnet generator, the inductances in a d-q reference frame are identical, so the electromagnetic torque can be expressed as:

$$T_e = \frac{3}{2} p \psi_m i_{sq} \tag{6}$$

where p is the number of pole pairs. Equation (6) shows that the generator torque is controlled directly by i_q component. The direct axis component of the current can be set to zero to minimize the current and hence minimizing resistive losses.

2.4. Power converter model

The PSMG is connected directly to the grid through B2B converter, where the converter is represented by a 3-phase controlled voltage source. These sources are driven by the control voltages of the PWM converters. Capacitor voltage variation represents the AC power flow in or out the converter. In this paper, we have used average converter model instead of the detailed converter model, where average converter model implies no switching, no change in circuit topology and it speeds up the simulation model. Neglecting converter losses the power balance equation can be obtained as follows [12]:

$$0 = P_{DC} + P_g + P_s \tag{7}$$

$$P_{DC} = V_{DC} i_{DC} = -CV_{DC}\frac{dV_{DC}}{dt} \tag{8}$$

$$\frac{dV_{DC}}{dt} = \frac{1}{CV_{DC}}\left(P_s - P_g\right) \tag{9}$$

where P_{DC} is the active power of the DC-link, P_g is the active power at the AC terminal of the grid side converter, P_s is the output active power of the PMSG, V_{DC} is the capacitor terminal voltage, i_{DC} is the capacitor current and C is the capacitance.

2.5. Braking resistor

The braking resistor is effective during normal operating conditions. When the voltage drops in the system, the terminal voltage of a wind turbine generator is reduced; also the active power that the wind turbine can export to the grid is reduced too. The energy imbalance appears in the wind turbine because the output power is quickly reduced by the inverter controller, while the input power extracted from the wind may not be reduced as quickly. This increase in energy in the DC link circuit cannot be exported. A braking resistor is placed in DC Link so as to dissipate this excess energy and restore the balance again. The braking resistor in variable speed drives balances the changes in output torque and prevent the DC link voltage to rise quickly [13]. This resistance is controlled using a power electronic switch as shown in Fig. 3.

2.6. Grid side converter model

The dynamic model of the grid connection when selecting a reference frame rotating synchronously with the grid voltage space vector is the following [14]:

$$v_{gd} = v_{cd} - R_g i_{gd} - L_{gd}\frac{di_{gd}}{dt} + \omega_g L_{gq} i_{gq} \tag{10}$$

$$v_{gq} = v_{cq} - R_g i_{gq} - L_{gq}\frac{di_{gq}}{dt} - \omega_g L_{gd} i_{gd} \tag{11}$$

where v_{gd}, v_{gq} are the grid voltages, v_{cd}, v_{cq} are the voltage components of the grid side converter, i_{gd}, i_{gq}, are the grid currents, R_g is the grid resistance, L_{gd}, L_{gq} are the grid inductances and ω_g is the grid frequency.

The active and reactive power in the synchronous reference frame is as follows:

$$P_g = \frac{3}{2}\left(v_{gd} i_{gd} + v_{gq} i_{gq}\right), Q_g = \frac{3}{2}\left(v_{gq} i_{gd} - v_{gd} i_{gq}\right) \tag{12}$$

As the d-axis of the reference frame is oriented along the grid voltage $v_g = v_{gd} + j.0$, the active and reactive powers can be expressed as [11]:

$$P_g = \frac{3}{2}v_{gd} i_{gd}, Q_g = -\frac{3}{2}v_{gd} i_{gq} \tag{13}$$

From equation 13, it can be deduced that the active and reactive power control can be achieved by controlling the direct and quadrature current components respectively.

3. Control Strategy

This system has three levels of the controller. The function of each level will be explained as:

3.1 Generator side converter

As described in Fig. 4 the goal of this controller is to work at the generator speed that extracts the maximum power from the wind without exceed allowable limits [11]. The parameters of PI controller are described in Appendix C.
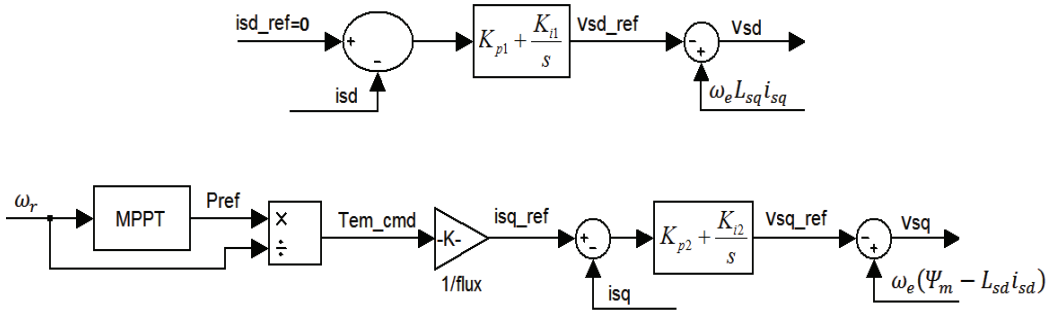
Fig. 4. Generator side converter control system.

3.2 Grid side converter

The aim of this controller is to maintain DC link voltage and frequency constant and to control the reactive power transferred to the network [9]. The structure the proposed controller is shown in Fig.5. The parameters of PI controller are described in Appendix C.
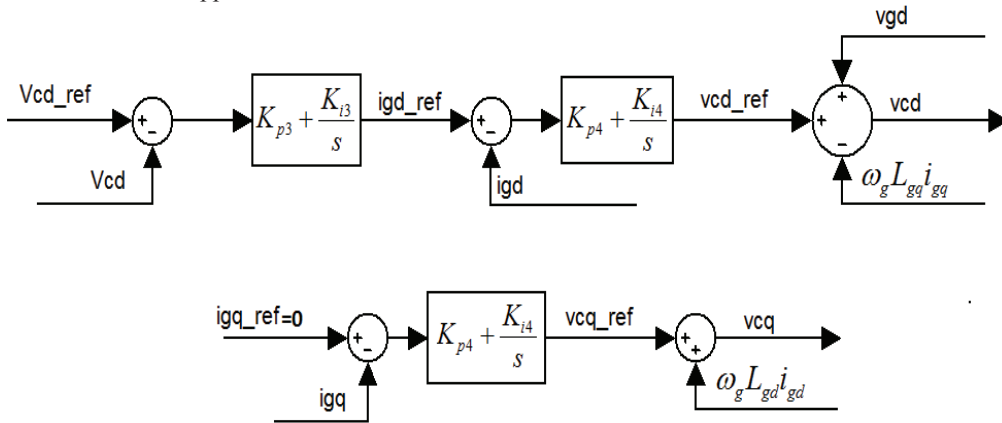
Fig. 5. Grid side converter control system.

3.3 Pitch angle control

This controller is necessary to control the rotational speed of the wind turbine. It activates in high wind speeds where the speed of the rotor exceeding the maximum rotor speed of the turbine via increase the blade pitch angle in order to reduce C_p and then reduces the power extracted from the wind [15].

4. Aggregate Modeling Techniques

As mentioned before this paper working on a comparison between the complete wind farm model and the other three aggregated models. Now each technique will be explained separately.

4.1 Multi full aggregate model using equivalent wind speed

In this technique the full wind farm is divided into groups, each group contains the same wind turbine types (same capacity and operational conditions), then each group is represented by equivalent wind turbine as shown in Fig. 6.
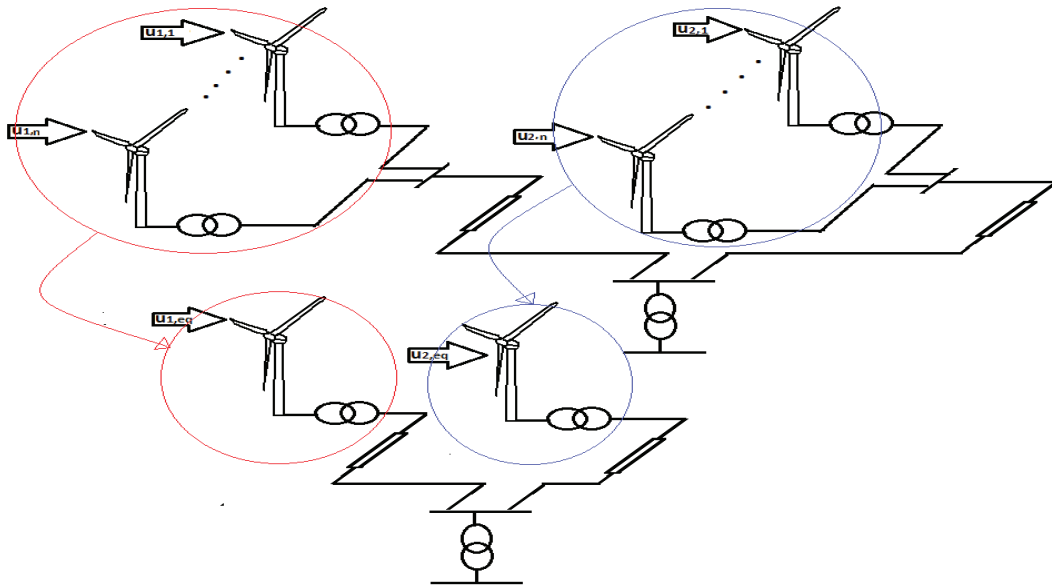

Fig. 6. Multi full aggregated model.

For identical wind turbines, equivalent wind turbine and equivalent generator presents n-times the size of individual wind turbines, as described in the following equation [5]:

$$S_{eq} = \sum_{j=1}^{n} S_j = nS_j \tag{14}$$

and the size of the equivalent compensating capacitors is given by:

$$C_{eq} = \sum_{j=1}^{n} C_j = nC_j \tag{15}$$

where n is the number of wind turbines in a wind farm, S_j is the rated apparent power of each wind turbines, S_{eq} is the rated apparent power of the equivalent wind turbine and C_j is the capacitance of each wind turbines.

The equivalent wind turbine or full aggregated wind turbine using equivalent wind speed (FWM_EWS) is consistent of one equivalent wind turbine and one equivalent generator (aggregated generator) with equivalent wind speed as shown in Fig. 7. The equivalent wind speed is derived from the power curve of the wind turbine as proposed in [5]:
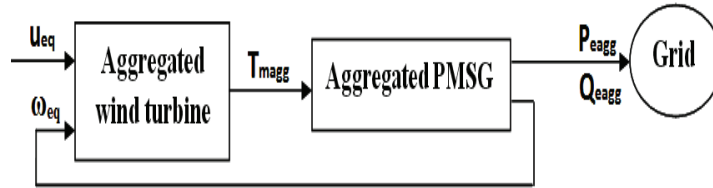
Fig. 7. Full aggregated model using equivalent wind speed.

4.2 Semi aggregated model

In the semi aggregated model (SAM), we have used the dynamic simplified model of each wind turbine with its speed to get the corresponding torques. Then, we sum up these torques to get the equivalent torque. Applying an equivalent torque to an equivalent generator model to get total active and reactive power exported to the grid system as shown in Fig.8.
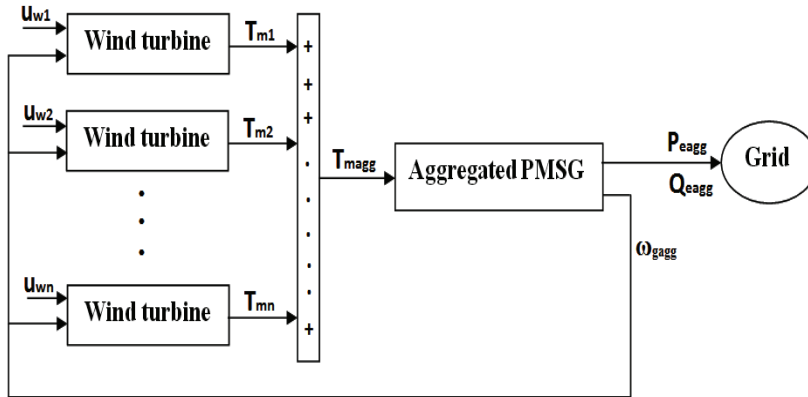

Fig .8. Semi aggregated model.

4.3 Mixed semi full aggregated model

This technique merges between MFAM_EWS and SAM. In this technique, we group wind turbines that have the same type, size and parameters to one equivalent wind turbine. Each equivalent wind turbine receives its own equivalent wind speed, then; the output of all equivalent wind turbines is aggregated and inserted it into the equivalent generator as shown in Fig. 9.
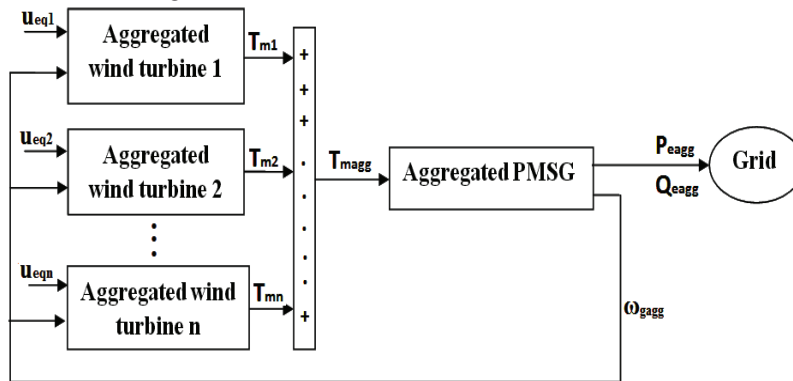

Fig. 9. Mixed semi full aggregated model.

5. Simulation Results

This research works on a large wind farm with a capacity of a 35 MW wind farm simulated by MATLAB/SIMULINK program. This wind farm consists of 15 PMSG wind turbines with different types of wind turbines. Fig. 1 presents 10 x 1.5 MW PMSG and 5 x 4 MW PMSG. These smaller farms connected to a 60 KV distribution system exporting power to a 220 KV grid through a 30 km 60 KV feeder. The rated speed of 1.5 MW wind turbine is 11 m/s and the rated speed of 4MW wind turbine is 13 m/s. The main parameters of each wind turbine type are provided in Appendix A.

The simulation studies the behavior of the wind farm integrated into the grid during steady state and transients. It compares between the complete wind farm and the aggregated models under two different operating conditions: normal condition (wind fluctuations) and fault condition (grid disturbances). The variable wind speeds received by the PMSG wind turbines are depicted in appendix B. 4 MW wind turbine has a higher elevation and exposed to higher wind speeds.

5.1 Normal operation

During normal operation, wind farm operates under wind speed fluctuations. The collective responses of the complete and the three aggregated wind farm models at the point of common coupling (PCC) during normal operation are shown in Fig. 10.
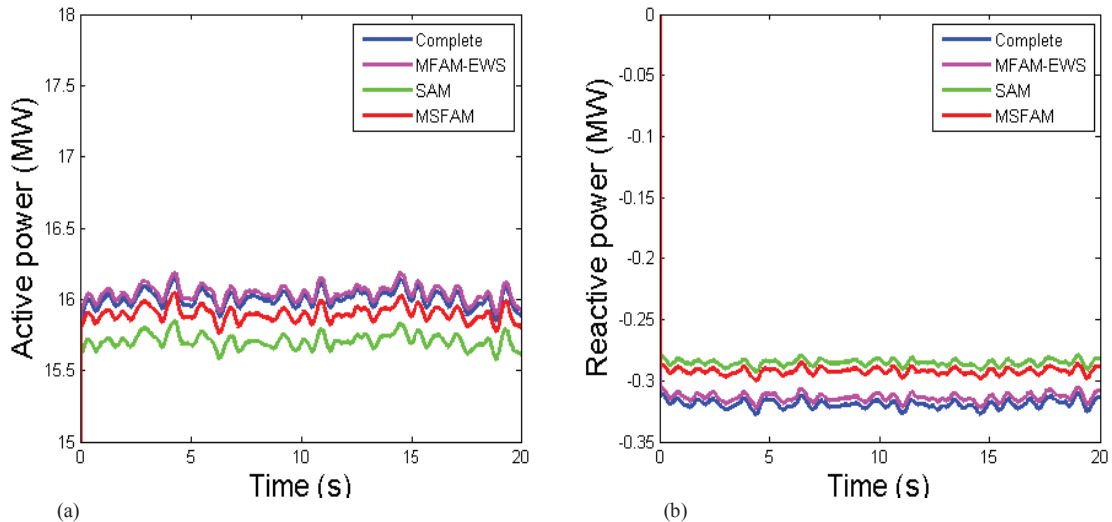

Fig. 10. (a) Active power at PCC during normal operation; (b) Reactive power at PCC during normal operation.

When the three aggregated modeling techniques are compared as depicted in Fig. 10(a, b), the multi full aggregated model using EWS achieve a better approximation of active and reactive power to the complete model. So we can depend on MFAM_EWS for representing the complete wind farm.

5.2 Grid disturbance

Assuming that the network voltage has dropped to its half value due to a fault for a period of 0.5 second at t=10s. Fig. 11 compares between the responses of the complete wind farm and the three aggregated models during fault condition.
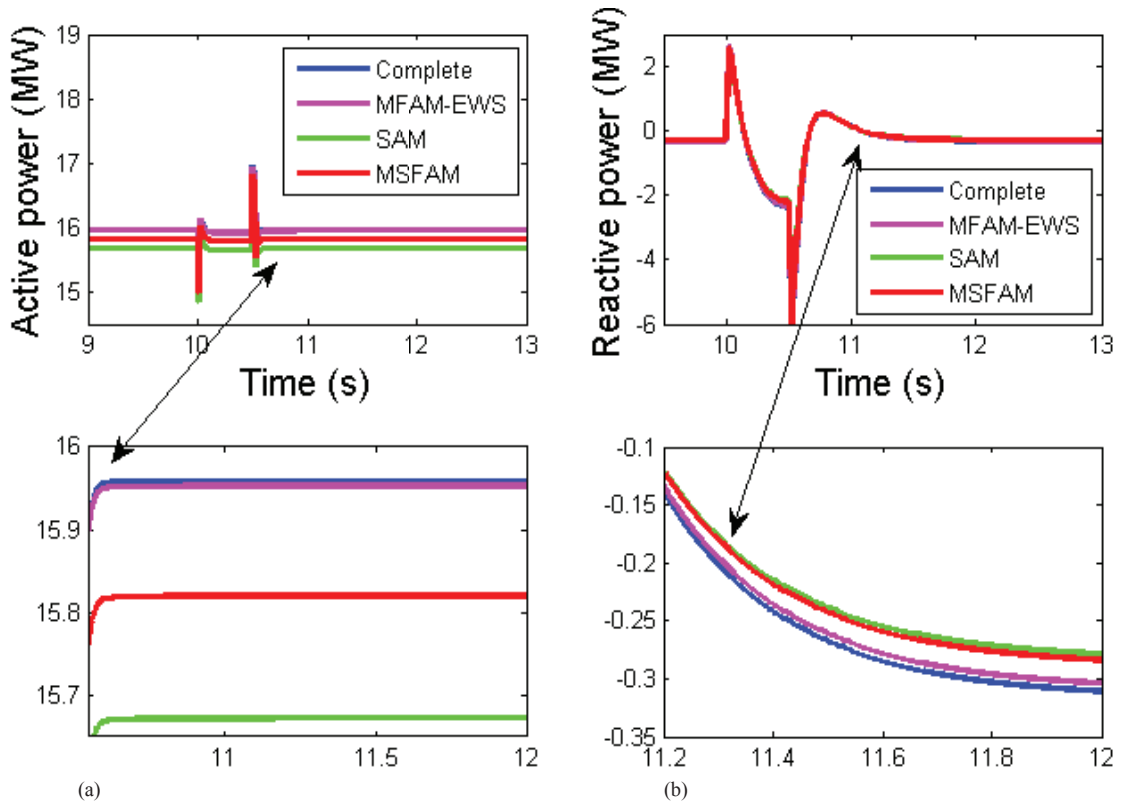
Fig. 11. (a) Active power at PCC during grid disturbance; (b) Reactive power at PCC during grid disturbance.

As shown in Fig. 11, it is clear that the MFAM_EWS is much closer to the complete wind farm during transient stability. This means that we can rely on MFAM_EWS even in cases of system dynamic disturbances, where it gives the nearest results in active and reactive power.

The comparison of accuracy in active and reactive power (P and Q) and computation simulation time for the complete and aggregated wind farm models are shown in Table 1and Table 2, respectively.

Table 1. Accuracy in closeness.

Aggregated model	MFAM-EWS	SAM	MSFAM
Accuracy in P	0.06%	1.82%	0.88%
Accuracy in Q	2.18%	10.28%	8.58%

Table 2. Computation time.

Aggregated model	complete	MFAM-EWS	SAM	MSFAM
Computation time (s)	203	36	31	26

This observation demonstrates that any of the three techniques consume lesser time than the complete model for the only 15 wind turbines used and MFAM_EWS has a high accuracy in approximation to the whole wind farm.

6. Conclusion

This research has presented three aggregated models of variable speed wind farm equipped with PMSG wind turbines for dynamic studies. This study includes: 1- multi full aggregated model using equivalent wind speed, 2- semi aggregated model and 3- mixed semi full aggregated model. A comparison between the complete wind farm and these aggregated models using MATLAB/SIMULINK program during normal and abnormal conditions are performed. As a conclusion multi full aggregated model using equivalent wind speed model has the highest accuracy to the complete model in steady and transient states as well as it consumes less time in the simulation compared with the complete model. A complete simulation of the system items has been discussed and presented.

References

[1] T. Ackermann, Ed.,Wind power in power systems, 2nd ed. John Wiley & Sons, 2012.
[2] J. Conroy, R. Watson. Aggregate modelling of wind farms containing full-converter wind turbine generators with permanent magnet synchronous machines: transient stability studies. IET, Renewable Power Generation, vol. 3, pp. 39 - 52, 2009.
[3] M. Ali, I.-S. Ilie, J.V. Milanovic, G. Chicco. Wind farm model aggregation using probabilistic clustering. IEEE Transactions on Power Systems, Vol 28, pp. 309 - 316, 2013.
[4] C. A. García, L. M. Fernández, F. Jurado. Evaluating reduced models of aggregated different doubly fed induction generator wind turbines for transient stabilities studies. Wind Energy, Vol 18, pp. 133 - 152, 2015.
[5] L. M. Fernandez, C. A. Garcia, J. R. Saenz, F.Jurado, "Equivalent models of wind farms by using aggregated wind turbines and equivalent winds. Energy Conversion and Management, vol. 50, pp. 691–704, 2009.
[6] C. N. Bhende, S. Mishra, S.G. Malla. Permanent magnet synchronous generator-based standalone wind energy supply system. IEEE Transactions on Sustainable Energy, pp. 361- 373, 2011.
[7]http://www.goldwindamerica.com/media/2012/12/Goldwind_15MW_Product_Brochure_2013.pdf
[8] T. L.Van, T. H. Nguyen, D. Lee. Advanced pitch angle control based on fuzzy logic for variable-speed wind turbine systems. IEEE Transactions on Energy Conversion, pp. 1-10, 2015.
[9] Md. E. Haque, M. Negnevitsky, K. M. Muttaqi. A Novel control strategy for a variable-speed wind turbine with a permanent-magnet synchronous generator. IEEE Transactions on Industry Applications, vol. 46, pp. 331 - 339, 2010.
[10] V. Akhmatov. Modelling and ride-through capability of variable speed wind turbines with permanent magnet generators. Wind Energy, Vol 9, Issue 4, pp. 313–326, 2006.
[11] J. Ivanqui, H. Voltolini, R. Carlson, and E. H. Watanabe , ""pq theory" control applied to wind turbine trapezoidal PMSG under symmetrical fault," IEEE International, Electric Machines & Drives Conference (IEMDC), pp. 534 – 540, 2013.
[12] F. Wu, X.-P. Zhangb, P. Ju. Small signal stability analysis and control of the wind turbine with the direct-drive permanent magnet generator integrated to the grid. Elsevier, Electric Power Systems Research 79, pp. 1661–1667, 2009.
[13] J. F. Conroy, R. Watson. Low-voltage ride-through of a full converter wind turbine with permanent magnet generator. IET, Renewable Power Generation, vol. 1, pp. 182-189, 2007.
[14] M. Chinchilla, S. Arnaltes, J. C. Burgos. Control of permanent-magnet generators applied to variable-speed wind-energy systems connected to the grid," IEEE Transactions on Energy Conversion, vol 21, pp. 130-135, 2006.
[15] F. M. González-Longatt, P. Wall, V. Terzija. A Simplified model for dynamic behavior of permanent magnet synchronous generator for direct drive wind turbines. IEEE Trondheim , PowerTech , pp. 1–7, 2011.

Appendix A. PMSG wind turbine parameters.

Parameter	Symbol	Value	Unit
Nominal voltage (L-L)	V_{nom}	690	V
Stator resistance	R_s	0.027	p.u.
Number of pole pairs	N_p	48	-
Rated speed	w_{PMSG}	125	rpm
Permanent flux	Ψ_m	1.18842	p.u.
Base frequency	f	50	Hz
Inertia of PMSG	H	0.685	s
C(dc-link capacitor)	C	10000	μF
Mutual inductance	L	0.51311	p.u.

Appendix B. Wind speeds incident on the wind turbines.

Wind turbine	Wind speed (m/s)	Wind turbine	Wind speed (m/s)
WT1	7	WT9	8.3
WT2	9	WT10	7.8
WT3	8	WT11	10
WT4	8.5	WT12	11
WT5	7.5	WT13	10.7
WT6	8.6	WT14	10.3
WT7	7.9	WT15	10.5
WT8	7.1		

Appendix C. PI controller parameters.

Parameter	Symbol	Value	Unit
Proportional gain of d-axis stator current regulator	K_{p1}	0.1361	p.u.
Integrating gain of d-axis stator current regulator	K_{i1}	2.7221	p.u.
Proportional gain of q-axis stator current regulator	K_{p2}	0.1361	p.u.
Integrating gain of q-axis stator current regulator	K_{i2}	2.7221	p.u.
Proportional gain of DC bus voltage regulator	K_{p3}	8	p.u.
Integrating gain of DC bus voltage regulator	K_{i3}	400	p.u.
Proportional gain of grid side converter current regulator	K_{p4}	0.83	p.u.
Integrating gain of grid side converter current regulator	K_{i4}	5	p.u.